Modelling of Color Scanners Using Neural Networks

H. J. Trussell

Dept. of Electrical and Computer Engineering
North Carolina State University
Raleigh, NC 27695-7911

M. J. Vrhel

Color Savvy Systems Ltd.
305 South Main Street
Springboro, OH 45066

Abstract

Since color scanners are not colorimetric, the optimal mapping from scanned values to colorimetric values is inherently nonlinear. Characterization of the scanner requires approximating this nonlinear mapping from the space of scanned values to a device independant color space. Neural networks are particularly suited to this task. Performance using an artificial neural network generated LUT is compared to that achieved by other commonly used methods.

1 Introduction

In order to reproduce consistent and accurate color with a scanner or printer, a mapping is needed from the device control values to a space that has a one-to-one mapping onto the CIE XYZ color space. This requirement leads to the definitions of device independent and device dependent color spaces.

A *device independent color space* is defined as any space that has a one-to-one mapping onto the CIE XYZ color space. Device independent values describe color for the standard CIE observer.

By definition, a *device dependent color space* cannot have a one-to-one mapping onto the CIE XYZ color space. In the case of a recording device, the device dependent values describe the response of that particular device to color. For a reproduction device, the device dependent values describe only those colors the device can produce.

Color scanners are not colorimetric. We define *colorimetric scanning* as the process of scanning or recording an image such that the CIE values of the image can be recovered from the recorded data. Scanner characterization is achieved by determining a mapping which maps the device dependent control values to a device independent color space (e.g. CIELAB). These mappings are nonlinear because of the linear characteristics of the actual hardware and, more importantly, because of the nonlinear transformation to the CIELAB space which models the sensitivity of the eye to color differences. It is noted that calibrating printers is even more nonlinear in practice. Typically, these mappings are implemented via a multidimensional look-up-table (LUT) in combination with some low order interpolation.

The neural network is inherently nonlinear when designed with nonlinear neural activation functions. The neural net approach has additional advantages in that it automatically achieves a certain degree of smoothness and does not require special programming on the part of the designer. The neural net approach is compared to standard methods including global linear and polynomial mappings, and a locally linear approximation method.

2 Color Scanner Characterization

Mathematically, the recording process of a scanner can be expressed as

$$\mathbf{c}_i = \mathcal{H}(\mathbf{M}^T \mathbf{r}_i)$$

where the matrix $\mathbf{M}$ contains the spectral sensitivity (including the scanner illuminant) of the three (or more) bands of the scanner, $\mathbf{r}_i$ is the spectral reflectance at spatial point i, $\mathcal{H}$ models any nonlinearities in the scanner (invertible in the range of interest), and $\mathbf{c}_i$ is the vector of recorded values.

The characterization problem is to determine the continuous mapping $\mathcal{F}_{scan}$ which will transform the recorded values to a CIE color space. In other words, determine the function $\mathcal{F}_{scan}$ such that

$$\mathbf{t} = \mathbf{A}^T \mathbf{L} \mathbf{r} = \mathcal{F}_{scan}(\mathbf{c})$$

for all $\mathbf{r} \in \Omega_r$, where Ω_r is the set of physically realizable reflectance spectra, the columns of matrix $\mathbf{A}$ contain the CIE XYZ color matching functions, and the diagonal matrix $\mathbf{L}$ represents the viewing illumination.

For the non-colorimetric scanner, there will exist spectral reflectances which look different to the standard human observer but when scanned produce the same recorded values. These colors are defined as being metameric to the scanner. Likewise, there will exist spectral reflectances which give different scan values and look the same to the standard human observer. While the latter can be corrected by the transformation $\mathcal{F}_{scan}$, the former cannot.

On the upside, there will always (except for degenerate cases) exist a set of reflectance spectra over which a transformation from scan values to CIE XYZ values will exist.

Printed images, photographs, etc. are all produced with a limited set of colorants. Reflectance spectra from such processes have been well modeled with very few (3-5) principal component vectors [1, 2, 3, 4].

When limited to such data sets it may be possible to determine a transformation $\mathcal{F}_{scan}$ such that

$$\mathbf{t} = \mathbf{A}^T \mathbf{L} \mathbf{r} = \mathcal{F}_{scan}(\mathbf{c})$$

for all $\mathbf{r} \in B_{scan}$ where B_{scan} is the subset of reflectance spectra to be scanned.

Look-up-tables, nonlinear and linear models for $\mathcal{F}_{scan}$ have been used to calibrate color scanners [5, 6, 7, 8]. In all of these approaches, the first step is to select a collection of color patches which span the colors of interest. Since the particular samples selected determine the characteristics of the mapping, the scanner characterization is usually identified with respect to the process which produced the samples. Ideally these colors should not be metameric in terms of the scanner sensitivities or to the standard observer under the illuminant for which the characterization is being produced. This constraint assures a one-to-one mapping between the scan values and the device independent values across these samples. In practice, this constraint is easily obtained. The reflectance spectra of these M_q color patches will be denoted by $\{\mathbf{q}\}_k$ for $1 \leq k \leq M_q$.

These patches are measured using a spectrophotometer or a colorimeter which will provide the device independent values

$$\{\mathbf{t}_k = \mathbf{A}^T \mathbf{q}_k\} \quad \text{for} \quad 1 \leq k \leq M_q.$$

Without loss of generality, $\{\mathbf{t}_k\}$ could replaced with any colorimetric or device independent values, e.g. CIELAB, CIELUV. The patches are also measured with the scanner to be calibrated providing $\{\mathbf{c}_k = \mathcal{H}(\mathbf{M}^T \mathbf{q}_k)\}$ for $1 \leq k \leq M_q$.

Mathematically, the characterization problem is: find a transformation $\mathcal{F}_{scan}$ where

$$\mathcal{F}_{scan} = \arg(\min_{\mathcal{F}} \sum_{i=1}^{M_q} ||\mathcal{F}(\mathbf{c}_i) - \mathcal{L}(\mathbf{t}_i)||^2)$$

where $\mathcal{L}(\cdot)$ is the transformation from CIEXYZ to the appropriate color space and $||.||^2$ is the error metric in the color space.

3 Artificial Neural Net

Because of its embedded nonlinearities, an artificial neural network (ANN) is well suited for the generation of the 3-D LUT in a scanner characterization problem. The mathematical description of the input-output relation for a single hidden layer neural network is given by [9]

$$\mathcal{L}(\mathbf{t}) = \mathbf{W}^1 \Phi(\mathbf{W}^0 \mathbf{c})$$

where $\Phi(\mathbf{u}) = [\phi_1(u_1), ..., \phi_N(u_N)]^T$, $\mathbf{u} = \mathbf{W}^0\mathbf{c}$, $\phi_i(\cdot)$ represents the neural activation function for the ith hidden neuron, and the bias in the neuron is accounted for by augmenting the vector $\mathbf{c}$.

The training of the network is a process of estimating the optimum weight matrices $\mathbf{W} = [\mathbf{W}^0, \mathbf{W}^1]$ which minimized the error on a given data set. In this case, the vector pairs $\{\mathbf{c}_i, \mathcal{L}(\mathbf{t}_i)\}$represent the input and output respectively. Once the network has been trained, the 3-D LUT is generated by evaluating the neural net at the RGB LUT grid points. These points may contain some data samples but since the number of samples is much smaller than the number of grid points, the performance of the LUT depends on the generalizing ability of the mapping obtained from the neural network.

Additionally, it must be possible to determine values for grid points in the table which may be outside the range of the scanned target data (i.e. the range of the scanned values $\mathbf{c}_i$ does not cover the entire space of possible scanned values). The neural net can easily be used to extrapolate values for the grid points that are beyond the range of the scanned target values. This is another advantage of the neural net approach. The extrapolation problem is a significant one for methods which reply on nearest neighbor interpolation/extrapolation. Even minor noise can cause large errors for these methods.

4 Example

A color target with 264 samples was measured with a three band (RGB) desktop color scanner. The CIELAB value for each sample was measured for D50 illumination. LUTs of size $N \times N \times N$ which map from the RGB output values to the CIELAB values were generated using four different methods. The size of the LUT was varied from $N = 4$ to $N = 32$. Linear interpolation was used to determine the values lying off the grid. It is noted that most sample points do not lie on the grid. The four methods were

1. A global linear fit was obtained between the RGB values and the CIE XYZ values. The fit mapped to CIEXYZ, but minimized the CIELAB ΔE error.

2. A global nonlinear fit was obtained which incorporated cross-polynomial terms of the scanned RGB data. The fit mapped to CIEXYZ but minimized the CIELAB ΔE error.

3. The N closest scanned values to the grid point were used to compute a locally linear fit for that region of RGB space.

4. An artificial neural network (ANN) was trained on half of the 264 samples and validated using the other half. A fully connected network with one hidden level was used with the signmoid activation function.

For each method, 3-D LUTs were generated by evaluating the function on the $N \times N \times N$ grid points. The scanned data was then fed into the LUT and the LUT output compared to the known LAB values for those 264 samples (training and validation sets). Linear interpolation was performed in the LUT. The results are given in Tables 1 and 2. Table 1 shows that in general overtraining is not a problem and that the number of neurons is not a critical parameter of the method. A graph of the maximum error verses LUT size is shown in Figure 1. The maximum is very important for evaluation of color fidelity since it is this error that is most disturbing to humans. Additionally, it should noted that ΔE errors under about three are undetectable by most observers. Thus, while the average errors indicate an undetectable difference, the maximum errors show differences that can be detected by the casual observer.

From the numerical results, it is clear that global linear and polynomial methods do not perform as well as the locally linear method or the ANN, and in fact the ANN provides the best results. The numerical results are confirmed by observation. However, an interesting observation of the various mappings is that the local linear method produces noticable discontinuities in the slope of the color mappings. This shows up as high local gradients which appear like contouring in quantization problems. Unfortunately, this effect cannot be reproduced in this printed version. The images can be obtained in the ftp directory /mbox/afs/eos.ncsu.edu/contrib/ftp/pub/hjt/profile. This effect is not surprising since the local linear method is susceptible to measurement noise. The neural network naturally produces a smooth function unless overtrained.

5 Conclusions

The problem of calibrating color scanners was defined mathematically. Various methods were compared in creating the characterization. From these preliminary results, the neural net approach is very promising for use in generating the 3-D LUT used in processing scanned data.

Num. Hidden Neurons	Average ΔE	Max ΔE
5	3.49	10.57
10	1.48	7.20
15	1.31	5.42
20	1.21	6.09
25	1.20	6.53

Table 1: ΔE results using ANN

References

[1] B. A. Wandell, "The Synthesis and Analysis of Color Images," *IEEE Trans. on Pattern Anal. and Machine Intell.*, vol. 9, no. 1, pp. 2-13, Jan. 1987.

[2] J. B. Cohen, "Dependency of the spectral reflectance curves of the munsell color chips," *Psychronomic Sci.*, vol. 1, pp. 369-370, 1964.

[3] J. Ho, B. Funt, and M. S. Drew, "Separating a color signal into illumination and surface reflectance components: theory and applications," *IEEE Trans. on Pattern Anal. and Machine Intell.*, vol. 12, pp. 966-977, Oct. 1990.

[4] M. J. Vrhel, R. Gershon, and L. S. Iwan, "Measurement and analysis of object reflectance spectra," *Color Res. Appl.*, vol. 19, pp. 4-9, Feb. 1994.

[5] P. C. Hung, "Colorimetric calibration in electronic imaging devices using a look-up table model and interpolations," *J. Electronic Imaging*, Vol. 2, pp. 53-61, Jan. 1993.

[6] H. R Kang and P. G. Anderson, "Neural network applications to the color scanner and printer calibrations," *J. Electronic Imaging*, Vol. 1, pp. 125-134, April 1992.

[7] H. Haneishi, T. Hirao, A. Shimazu, and Y. Mikaye, "Colorimetric precision in scanner calibration using matrices," in *Proc. Third IS&T/SID Color Imaging Conference: Color Science, Systems and Applications*, Nov. 1995, pp. 106-108.

[8] H. R. Kang, "Color Scanner Calibration," *J. Imaging Sci. Technol.*, Vol. 36, pp. 162-170, Mar./Apr. 1992.

[9] S. Haykin, *Neural Networks,* MacMillan, New York, 1994.

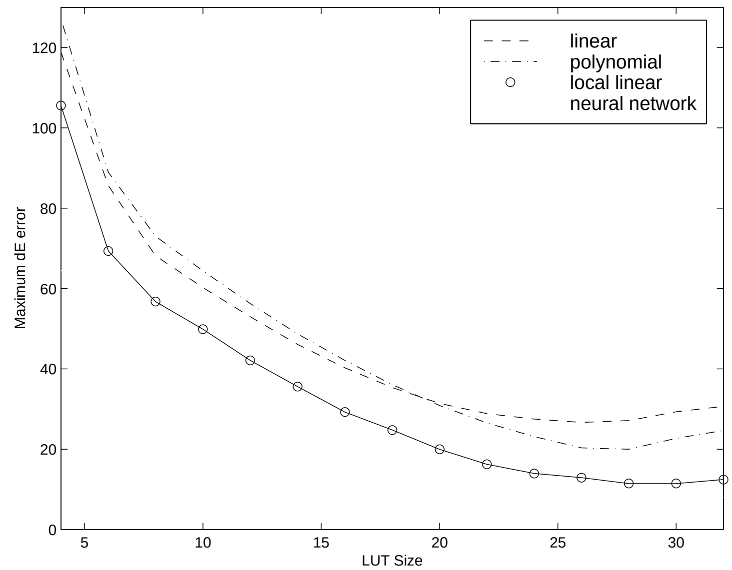

Figure 1: Maximum Error versus LUT Size

LUT size	Linear		Polynomial		Local Linear		Neural Network	
	ΔE avg	ΔE max	ΔE avg	ΔE max	ΔE avg	ΔE max	ΔE avg	ΔE max
4	30.22	118.85	31.38	127.10	26.84	105.57	19.13	64.64
6	16.22	85.63	16.29	88.94	13.80	69.36	10.22	46.04
8	12.34	68.16	11.93	73.01	9.56	56.74	6.68	35.52
10	10.04	60.25	9.37	64.39	7.27	49.88	4.98	29.24
12	8.17	52.99	7.27	56.28	5.63	42.12	3.89	26.22
14	6.88	46.10	5.98	48.71	4.49	35.61	3.27	22.73
16	6.04	40.29	5.12	42.12	3.81	29.26	2.89	20.28
18	5.51	35.35	4.59	36.10	3.26	24.79	2.51	17.50
20	5.16	31.43	4.20	30.90	2.85	19.96	2.23	15.09
22	4.91	28.85	3.90	26.56	2.57	16.25	2.01	12.95
24	4.79	27.52	3.79	23.13	2.41	13.96	1.88	11.26
26	4.65	26.69	3.65	20.34	2.25	12.93	1.74	9.66
28	4.54	27.14	3.53	20.00	2.16	11.45	1.67	8.99
30	4.50	29.33	3.49	22.70	2.10	11.44	1.65	8.54
32	4.49	30.68	3.46	24.68	2.10	12.46	1.62	8.07
INF	4.38	28.33	3.28	19.37	1.93	10.02	1.38	6.49

Table 2: ΔE results using half of data for training and half for testing